Virus Evolution, 2024, **10(1)**, veae006
DOI: https://doi.org/10.1093/ve/veae006
Advance Access Publication 21 February 2024
Research article

Within-host evolution of SARS-CoV-2: how often are *de novo* mutations transmitted from symptomatic infections?

Chapin S. Korosec,[1,2,§,*] Lindi M. Wahl,[3,‡] and Jane M. Heffernan[1,2]

[1]Modelling Infection and Immunity Lab, Mathematics and Statistics, York University, 4700 Keele St, Toronto, ON M3J 1P3, Canada, [2]Centre for Disease Modelling, Mathematics and Statistics, York University, 4700 Keele St, Toronto, ON M3J 1P3, Canada and [3]Applied Mathematics, Western University, 1151 Richmond St, London, ON N6A 5B7, Canada
[§]https://orcid.org/0000-0001-5137-2195
[‡]https://orcid.org/0000-0003-1163-0940
*Corresponding author: E-mail: chapinSkorosec@gmail.com

Abstract

Despite a relatively low mutation rate, the large number of severe acute respiratory syndrome coronavirus 2 (SARS-CoV-2) infections has allowed for substantial genetic change, leading to a multitude of emerging variants. Using a recently determined mutation rate (per site replication), as well as within-host parameter estimates for symptomatic SARS-CoV-2 infection, we apply a stochastic transmission-bottleneck model to describe the survival probability of *de novo* SARS-CoV-2 mutations as a function of bottleneck size and selection coefficient. For narrow bottlenecks, we find that mutations affecting per-target-cell attachment rate (with phenotypes associated with fusogenicity and ACE2 binding) have similar transmission probabilities to mutations affecting viral load clearance (with phenotypes associated with humoral evasion). We further find that mutations affecting the eclipse rate (with phenotypes associated with reorganization of cellular metabolic processes and synthesis of viral budding precursor material) are highly favoured relative to all other traits examined. We find that mutations leading to reduced removal rates of infected cells (with phenotypes associated with innate immune evasion) have limited transmission advantage relative to mutations leading to humoral evasion. Predicted transmission probabilities, however, for mutations affecting innate immune evasion are more consistent with the range of clinically estimated household transmission probabilities for *de novo* mutations. This result suggests that although mutations affecting humoral evasion are more easily transmitted when they occur, mutations affecting innate immune evasion may occur more readily. We examine our predictions in the context of a number of previously characterized mutations in circulating strains of SARS-CoV-2. Our work offers both a null model for SARS-CoV-2 mutation rates and predicts which aspects of viral life history are most likely to successfully evolve, despite low mutation rates and repeated transmission bottlenecks.

Keywords: virus evolutionary dynamics; viral evolvability; virus life history evolution; evolution of immune escape; SARS-CoV-2; COVID-19; variants of concern; transmission dynamics; de novo mutations; bottleneck dynamics; viral evolution.

1. Introduction

The emergence and rapid spread of severe acute respiratory syndrome coronavirus 2 (SARS-CoV-2) in late 2019 marked the onset of an unprecedented global health crisis. The evolution of SARS-CoV-2 variants of concern (VOC) has since posed immense challenges to public health, impacting societies worldwide. A mutant lineage nomenclature based on phylogenetic framework was developed, which enabled tracking single-nucleotide polymorphisms (SNPs), as well as linking specific SNPs to changes in viral fitness traits (Rambaut et al., 2020). Currently, the XBB.1.5 variant, a recombinant of two BA.2 Omicron subvariants, is the predominant variant of concern circulating globally. XBB.1.5 has 'high' growth advantage and 'moderate' ability for immune escape as compared to previous omicron subvariants, as determined by The World Health Organization (XBB.1.5 Updated Risk Assessment, 2023).

The mutation rate of SARS-CoV-2 has been estimated using genome sequencing and phylogenetics and is relatively low for viral pathogens (Amicone et al., 2022). Since case counts worldwide exceed 750 million cumulative infections to date (World Health Organization, 2023), however, SARS-CoV-2 has accrued substantial genetic diversity (Hadfield et al., 2018). At the population level, much attention has been focused on quantifying between-host diversity and determining current SARS-CoV-2 epidemiological traits (Zhang et al., 2020; Salzberger et al., 2021; Tian et al., 2022). However, novel mutations first occur within a single individual, and thus, methodology capable of predicting within-host diversity and forecasting the transmission probability for novel mutations is essential for predicting the emergence of future SARS-CoV-2 VOC. The ongoing threat to public health from SARS-CoV-2 evolution necessitates a need for 'a full model incorporating within-host evolutionary dynamics and transmission'

(Lythgoe et al., 2021) to predict how new mutations arise and are transmitted and to predict the rate at which new variants will arise, so that best-informed interventions can be enacted.

We have developed a data-driven model describing SARS-CoV-2 within-host evolutionary dynamics. The model is used to compute the probability that at least one copy of a novel mutation arising in a host survives to be transmitted to a new host. We quantify the fate of neutral mutations, as well as mutations leading to immune escape, increased transmissibility, binding affinity, and replication. For each mutant lineage, we explore how bottleneck size and mutant fitness affect the transmission probability. Finally, we contextualize our model predictions with data from known SARS-CoV-2 mutations that have been quantitatively linked to phenotypic changes in viral fitness.

2. Methods

Within-host modelling of SARS-CoV-2 has helped to elucidate the molecular mechanisms driving SARS-CoV-2 transmission as well as immunological responses from vaccines and infection (Gholami et al., 2023; Padmanabhan, Desikan and Dixit, 2022; Lin et al., 2022; Korosec et al., 2022; Moyles, Korosec and Heffernan, 2023; Farhang-sardroodi et al., 2021; Matveev et al., 2023), as well as offer key insights into the potential implications of public health burden and interventions (Betti et al., 2021; Johansson et al., 2021; Le Rutte et al., 2022). In this work, our within-host target-cell-limited model is similar in structure to models of within-host infection that have been used to quantify the dynamics of SARS-CoV-2 within an infected individual (Néant et al., 2021; Jones et al., 2021; Goyal, Cardozo-Ojeda and Schiffer, 2020) and estimate viral fitness traits for a number of SARS-CoV-2 VOCs (i.e. attachment rate and budding rate) (Korosec et al., 2023; Néant et al., 2021; Gonçalves et al., 2020; Gonçalves et al., 2021; Perelson and Ke, 2021). Our model is given by the following equations:

$$\text{Target cells}: \frac{dy_T}{dt} = -\alpha y_T v, \tag{1a}$$

$$\text{Eclipse stage 1}: \frac{dy_1}{dt} = \alpha y_T v - (D + kE) y_1, \tag{1b}$$

$$\text{Eclipse stage 2...k}: \frac{dy_j}{dt} = kE y_{j-1} - (D + kE) y_j, \; j = 2...k, \tag{1c}$$

$$\text{Budding}: \frac{dy_B}{dt} = kE y_k - D y_B, \tag{1d}$$

$$\text{Infectious virus}: \frac{dv}{dt} = \epsilon B y_B - \alpha y_T v - Cv. \tag{1e}$$

A schematic of our in-host model of SARS-CoV-2 infection with three eclipse stages (Eq. (1)) is shown in Fig 1A. A schematic of the stochastic model employed to determine transmission probabilities of rare mutations is shown in Fig 1B. Parameters for 'wildtype' SARS-CoV-2 infection (Section S1.2 and Discussion) are determined from the literature and are listed in Table 1. We note that the parameters used in this model correspond to predominantly severe SARS-CoV-2 infections, estimated from a dataset composed of mostly hospitalized individuals. Using these parameters, our estimate for the within-host reproduction number, R_0, for these severe infections is 19.0.

The within-host diversity of SARS-CoV-2 is relatively low, with narrow transmission bottlenecks (Braun et al., 2021; Martin and Koelle, 2023; Lythgoe et al., 2021; Bendall et al., 2023). This small bottleneck size leads to low diversity at the time of transmission, whereby the majority variant is typically transmitted to a new host (Bendall et al., 2023), and thus, the emergence and spread of a *de novo* mutation will be a statistically rare event. While modelling and prediction of rare impactful events can be approached through computational simulations (Van Egeren et al., 2021), we follow Sigal, Reid and Wahl (2018) in developing a rigorous within-host mathematical model of the underlying process. This allows for a full analytical exploration of the factors driving the emergence of a VOC. Following Sigal, Reid and Wahl (2018), we develop a model for the wildtype population dynamics (Section S1.1) and a stochastic model for the introduction of new and rare viral variants (Section S1.3). Model parameter values are informed from the literature (Section S1.2). The full stochastic model is given by the following pgf, and we direct the reader to Supplementary Information for further description,

$$\begin{aligned}\frac{\delta G}{\delta t} &= (A(t)x_2 + C - (A(t) + C)x_1)\frac{\delta G}{\delta x_1} \\ &+ \sum_{i=1}^{k}(-(kE + D)x_{i+1} + kEx_{i+2} + D)\frac{\delta G}{\delta x_{i+1}} \\ &+ (Bx_1x_B + D - (D + B)x_B)\frac{\delta G}{\delta x_B}.\end{aligned} \tag{2}$$

To capture the emergence of a new mutant and the growth of the mutant and wildtype population, we couple the stochastic and deterministic models (Section S1.4). Using the percent change in the basic reproduction number as a metric of fitness of *de novo* advantageous mutants, we define life history and immune escape traits that can affect the emergence and transmissibility of a mutant strain (Section S1.5). For each mutant arising at each time t_m, full stochastic dynamics are followed up to the point of transmission. Finally, we determine the probability that a new variant that arises at time $0 < t_m < \tau$ can be transmitted at time τ, the time of the transmission bottleneck event (Section S1.6), which is assumed to occur at the time of peak viral load of the neutral strain.

We note that the modelling framework presented here does not explicitly model the immune response. The immune response is instead included in model parameters, for example, reflecting virus neutralization by antibodies (C), infected cell killing by cytotoxic T-lymphocytes (D), and the ability of the virus to infect a target cell modified by interferon (α). Furthermore, we make the simplifying assumption that these parameters do not vary with time. This is reasonable since we model the in-host infection only to the point of peak viral load, and the adaptive immune response typically plays a limited role before this time (Sette and Crotty, 2021). Due to this early timing, and consistent with other target-cell-limited models of SARS-CoV-2 infection (Korosec et al., 2023; Néant et al., 2021; Ciupe and Tuncer, 2022), we also do not consider susceptible target cell replenishment.

3. Results

3.1 Neutral strain bottleneck dynamics for narrow bottlenecks and selective coefficient

A schematic of the deterministic model with three eclipse stages (Eq. (S1)) is shown in Fig 1A, and a schematic of the stochastic model is shown in Fig 1B. Parameters for the wildtype strain are determined from the literature and are listed in Table 1.

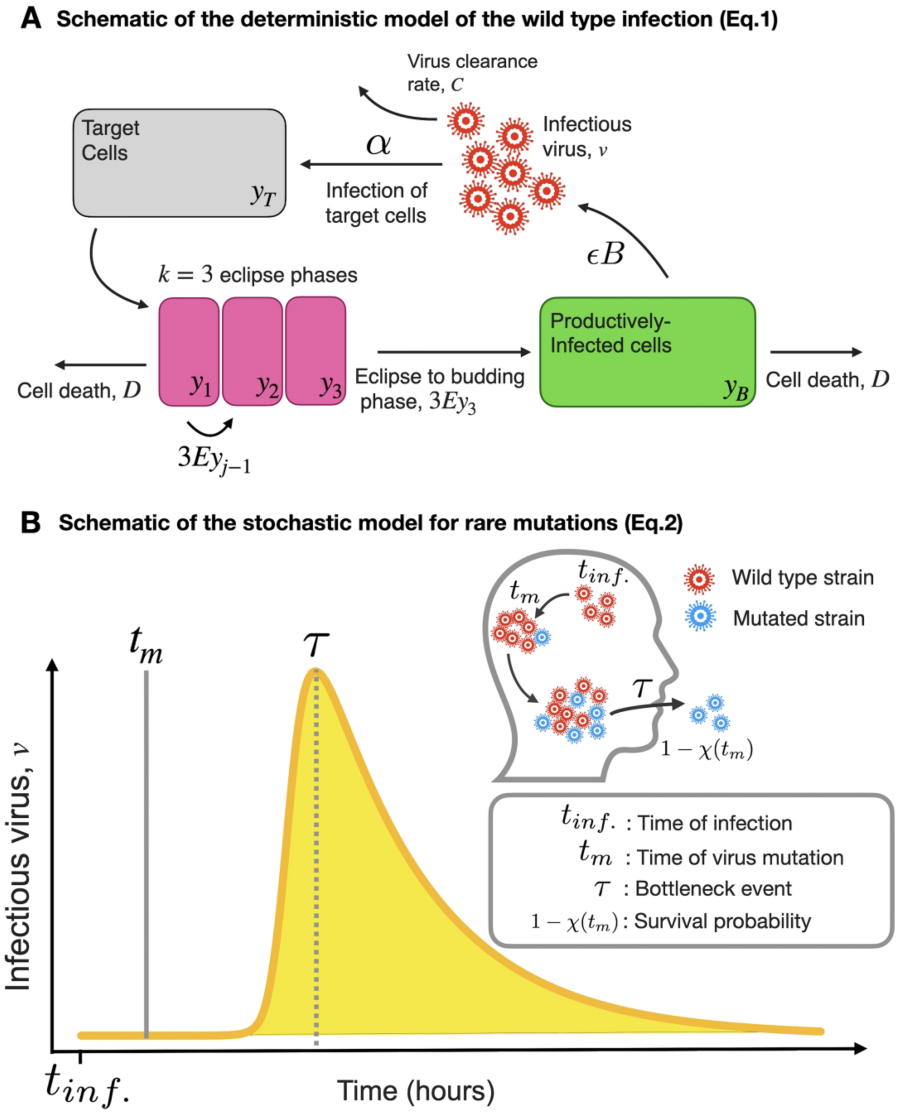

Figure 1. (A) Schematic of the deterministic model of the wildtype infection (Eq. (1)) described in Section S1.1. (B) Schematic of the stochastic model for rare mutations (Eq. (2)) described in Sections S1.3 and S1.6.

The infection time course for the wildtype strain is shown in Figure 2A. We note that the viral load peaks 6 days post-infection and decays over the course of several weeks, consistent with the predominantly severe SARS-CoV-2 cases in the dataset that informed these parameter values. We also note that the susceptible target cell population, representing epithelial cells of the upper respiratory tract, is reduced to near zero at the peak of the infection. This is consistent with empirical observations in murine influenza, in which complete desquamation of epithelial cells occurs several days post-infection (Ramphal et al., 1979), as well as for coronavirus disease 2019 (COVID-19) in humans where desquamation of lungs and airway (Liu et al., 2021; Schaefer et al., 2020) as well as epithelial olfactory cells (Vaira et al., 2020) have all been observed.

The rare mutations studied in the stochastic model can affect any of five viral traits: attachment, budding, viral clearance, infected cell death, and eclipse phase timing, captured in parameters α, B, C, D, and E, respectively. Figure 2B illustrates the percent change in the wildtype parameter value that is required to achieve a specific increase in R_0 for the variant strain. We note that very large increases in the eclipse rate E (reflecting substantial reductions in the eclipse phase duration) are needed to achieve even moderate changes in R_0. This indicates that the delay during the eclipse phase, 4.8 h on average, does not substantially reduce R_0 at these parameter values. For example, even if the eclipse duration is reduced to zero (letting the rate E approach ∞), R_0 is increased by less than 10 per cent (Fig. 3). The attachment rate, α, displays a similar but milder trend; for example, doubling α increases R_0 by only 50 per cent. The three remaining parameters show increases in R_0 that are quite similar in magnitude to the respective percentage change in the parameter value. These considerations will become important in gaining a qualitative understanding of the results to follow.

Fig. S1A and S1B displays the survival probability of a *de novo* mutation (P_s, Eq. (S5)) and the rate at which surviving lineages are created (κ, Eq. (S6)) respectively, for neutral mutations. We note that the neutral strain reproduces the 'hockey stick' pattern found for neutral mutations in influenza A (Sigal, Reid and Wahl, 2018), as shown in the semi-log plot of P_s (Fig. S1B).

Table 1. Parameter estimates for the wildtype (deterministic) model (Eq. (1)) and the mutant (stochastic) model (Eq. (2)).

Parameter	Units	Definition	Estimate	Reference
Deterministic model, parameters for the wildtype strain				
α	mL d^{-1} copies^{-1}	Per target cell attachment rate	7.9×10^{-5}	(Korosec et al., 2023)
ϵ	Unitless	Fraction of infectious virus	10^{-4}	(Gonçalves et al., 2021; Néant et al., 2021)
ϵB	copies d^{-1} d^{-1} cell^{-1}	Infectious virus budding rate	15.7	(Korosec et al., 2023)
C	d^{-1}	Clearance rate	15	(Korosec et al., 2023; Goyal, Cardozo-Ojeda and Schiffer, 2020)
D	d^{-1}	Infected cell death rate	0.32	(Korosec et al., 2023), (Cao et al., 2021)[b]
E	d^{-1}	Eclipse rate	5	(Korosec et al., 2023; Agostini et al., 2018; Ghosh et al., 2020)
k	Unitless	Stages in eclipse phase	3	(Korosec et al., 2023)
R_0^N	Unitless	Reproduction number for the neutral strain	19.0	(Korosec et al., 2023)
$y_T(0)$	Cell ml^{-1}	Initial number of target cells	1.33×10^5	(Néant et al., 2021; Gonçalves et al., 2020; Baccam et al., 2006)
$y_k(0)$	Cell ml^{-1}	Initial number of cells in the eclipse phase	0	N/A
$y_B(0)$	Cell ml^{-1}	Initial number of infected cells	1/30	(Néant et al., 2021)
$v(0)$	Copies ml^{-1}	Initial number of infectious virus	0	N/A
Stochastic model parameters				
Λ	Virus particles	Bottleneck size: number of viruses founding infection	1–50[a]	(Wang et al., 2021; Braun et al., 2021; Martin and Koelle, 2023; Lythgoe et al., 2021; Bendall et al., 2023)
μ	nt^{-1}cycle^{-1}	Mutation rate (per site replication)	1.3×10^{-6}	(Amicone et al., 2022)
τ	h	Disease transmission time	144	Calculated

All parameters used in this work are SARS-CoV-2 specific and sourced from the previously published literature.
[a]Total range explored in this work, motivated from all cited references.
[b]Reference to the severe-case infected cell removal rate from Cao et al. (2021)

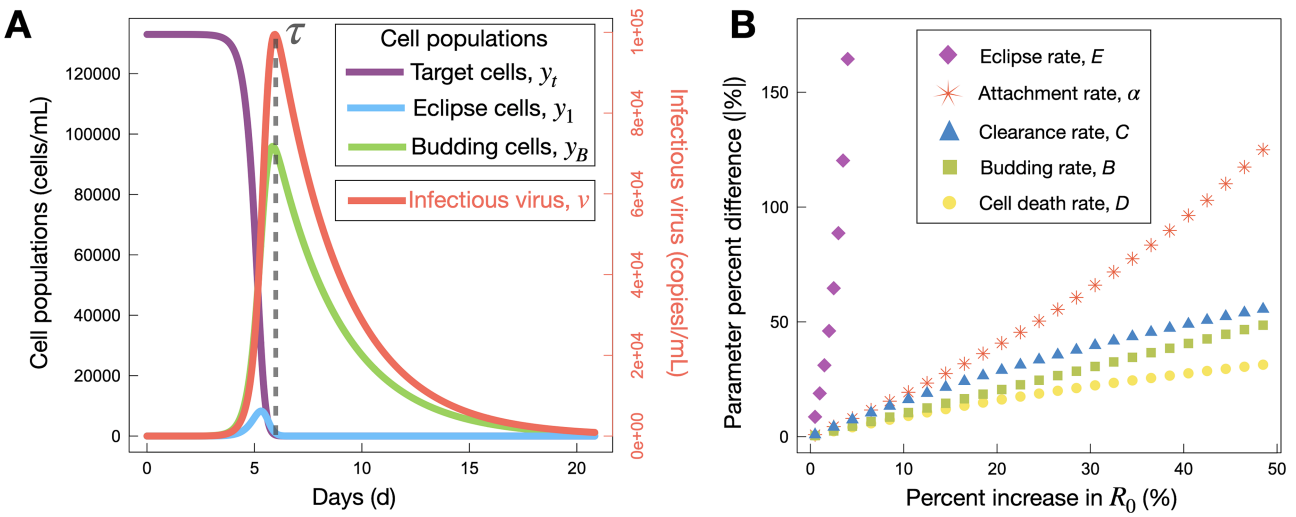

Figure 2. Wildtype dynamics. (A) Time course of the wildtype infection (Eq. (1)). Cell populations are plotted against the left-hand axis, while infectious virions are plotted against the right-hand axis. The grey dashed line indicates the transmission bottleneck time, τ, which is fixed for all transmission events to the time of peak infectious virus. (B) Percent change in model parameters required to achieve a specific percent increase in the reproductive ratio, R_0. Wildtype parameters are listed in Table 1.

3.2 Variant dynamics with narrow bottlenecks ($\Lambda = 1$)

We begin by considering the fate of rare mutations for narrow bottlenecks of size $\Lambda = 1$. As seen in Fig 3 (y-intercept), we find that the probability of transmitting at least one copy of a specifc mutation (Π, Eq. (S9)) is approximately 5.2×10^{-7} for a neutral mutation with a transmission bottleneck of size one.

Fig 3 displays our predictions of Π for variants that carry adaptive (beneficial) mutations affecting different traits. We see that for the same increase in R_0, mutations affecting the eclipse phase timing have a high transmission probability, relative to other traits, while mutations affecting the death rate of infected cells are least likely to survive transmission. Mutations in α, C, and B lead to a similar increase in Π as a function of R_0. We note that mutations in E are limited to a maximum increase in R_0^N of 6.5 per cent, as further increases in R_0^N would require extreme changes in eclipse phase timing (Fig. 2B). In Fig. S2, we include a plot of Π as a function of the percent increase in each parameter. Here, we see that the growth in Π is near exponential with percent change in parameters C and D, but slightly sub-exponential with parameters α, D, and E. Overall, if we compare parameter changes that produce the same percent change in rate, differences in Π are more modest than when comparing parameter changes that produce the same percent change in R_0.

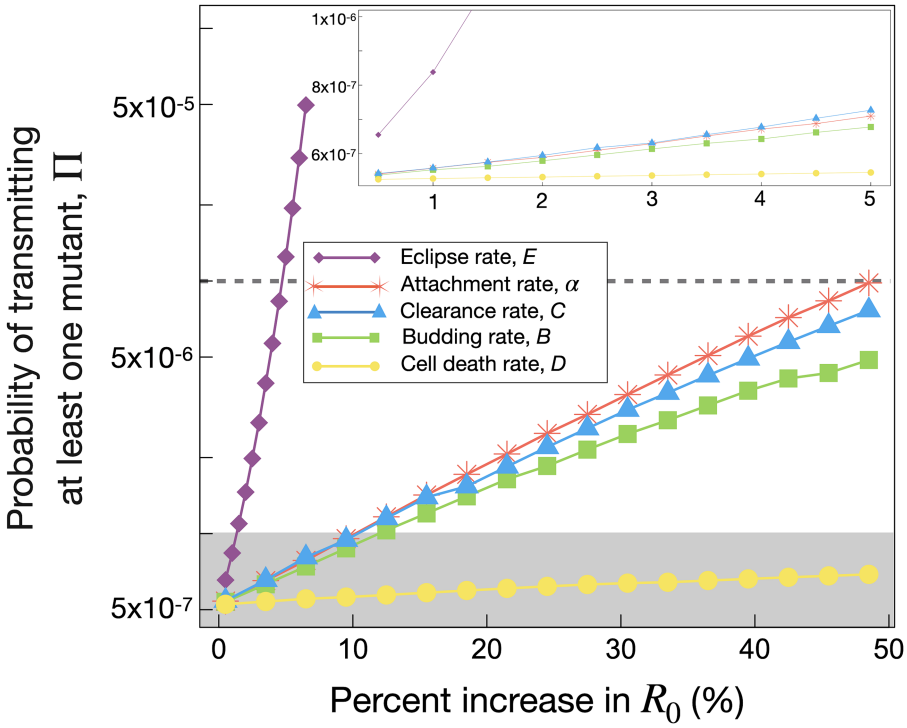

Figure 3. Probability of transmitting at least one copy of a specific mutation, Π (Eq. (S9)), as a function of percent increase in R_0 (Eq. (S4)), for a bottleneck of size $\Lambda = 1$. Results for mutations affecting parameters E, α, C, B, and D are shown as diamonds, stars, triangles, sqaures, and circles, respectively. Grey box and the inset show previously determined parameter ranges in Π, while the grey line at $1x10^{-5}$ marks the approximate value of the SARS-CoV-2 substitution rate (Section 4).

For completeness, Fig. S1C and S1D displays P_s (Eq. (S5)) and κ (Eq. (S6)) for mutations leading to a 5 per cent R_0^N increase, for each model parameter. All mutations lead to an increase in P_s and κ for all t_m as compared to neutral mutations. Figs. S3 and S4 show the increase in P_s and κ, respectively, for all mutation parameters and all selective coefficients.

3.3 Changes in variant dynamics with transmission bottleneck size

As described in the Section 1, estimates of the transmission bottleneck size, Λ, for SARS-CoV-2 include a range of values. Figure 4 displays Π as a function of Λ for mutations leading to an increase in R_0 of 0.5 per cent (Fig. 4A), 5.0 per cent (Fig. 4B), or 50 per cent (Fig. 4C). Overall, we see that the probability that a new variant is transmitted increases with bottleneck size.

An R_0 increase of 0.5 per cent leads to a similar increase in Π with Λ for all mutation types, with transmission probabilities close to those expected for a neutral mutation. When the variant has a 5.0 per cent increase in R_0, a clear hierarchy of parameter influence on Π as a function of Λ emerges. As seen before, mutations affecting the eclipse phase timing are the most likely to be transmitted, irrespective of the bottleneck size. For very fit variants (50% increase in R_0), eclipse phase mutations are no longer realistic as described previously. Here, mutations affecting the attachment rate α or clearance rate C are found to have a higher probability of transmitting. Mutations in the budding rate B have an intermediate effect on Π, while mutations affecting the cell death rate, D, appear to offer a limited transmission advantage compared to the neutral strain. This final result is surprising, given that the mutation in question confers a 1.5 times increase in R_0 when compared to the wildtype. To further illustrate the selective advantage of each mutation over the neutral strain, in Fig. S5, we report the ratio of the mutant Π to that of the neutral strain for each parameter. Notably, we find that with a selective coefficient of only 5.0 per cent, E has a 20x higher probability of transmitting at narrow bottlenecks, whereas the selective coefficient needs to be as high as 50 per cent for mutations in α and B to have a 20x higher probability of transmitting at narrow bottlenecks. In Fig. S6, we examine these trends in greater detail, combining results for Π as a function of both R_0 and bottleneck size. We see that the increase in Π is roughly exponential with mutant fitness, for mutations affecting α, B, C, and D, and find that Π scales faster than exponentially as a function of R_0 for mutations affecting E.

4. Discussion

Pathogens face significant selective pressure to proliferate within the host, whereas host defensive mechanisms are geared towards impeding pathogen replication. This ongoing conflict between the host and pathogen creates an arms race, resulting in diverse outcomes that can either enhance or diminish virulence (Longdon et al., 2015). In this study, we used a stochastic model to explore the fate of neutral and advantageous SARS-CoV-2 mutations, where the wildtype strain was calibrated to SARS-CoV-2 within-host viral load data collected from predominantly hospitalized individuals between February 2020 through to February 2021 in Berlin, Germany (Jones et al., 2021).

Our computed probabilities of transmitting at least one copy of a specific mutation, Π, compare well to recent estimates of SARS-CoV-2 transmission probabilities from simulation. In particular, Van Egeren et al. (2021) explore the probability of variant transmission as a function of increased infection period through intrahost viral dynamic simulations. They find that approximately

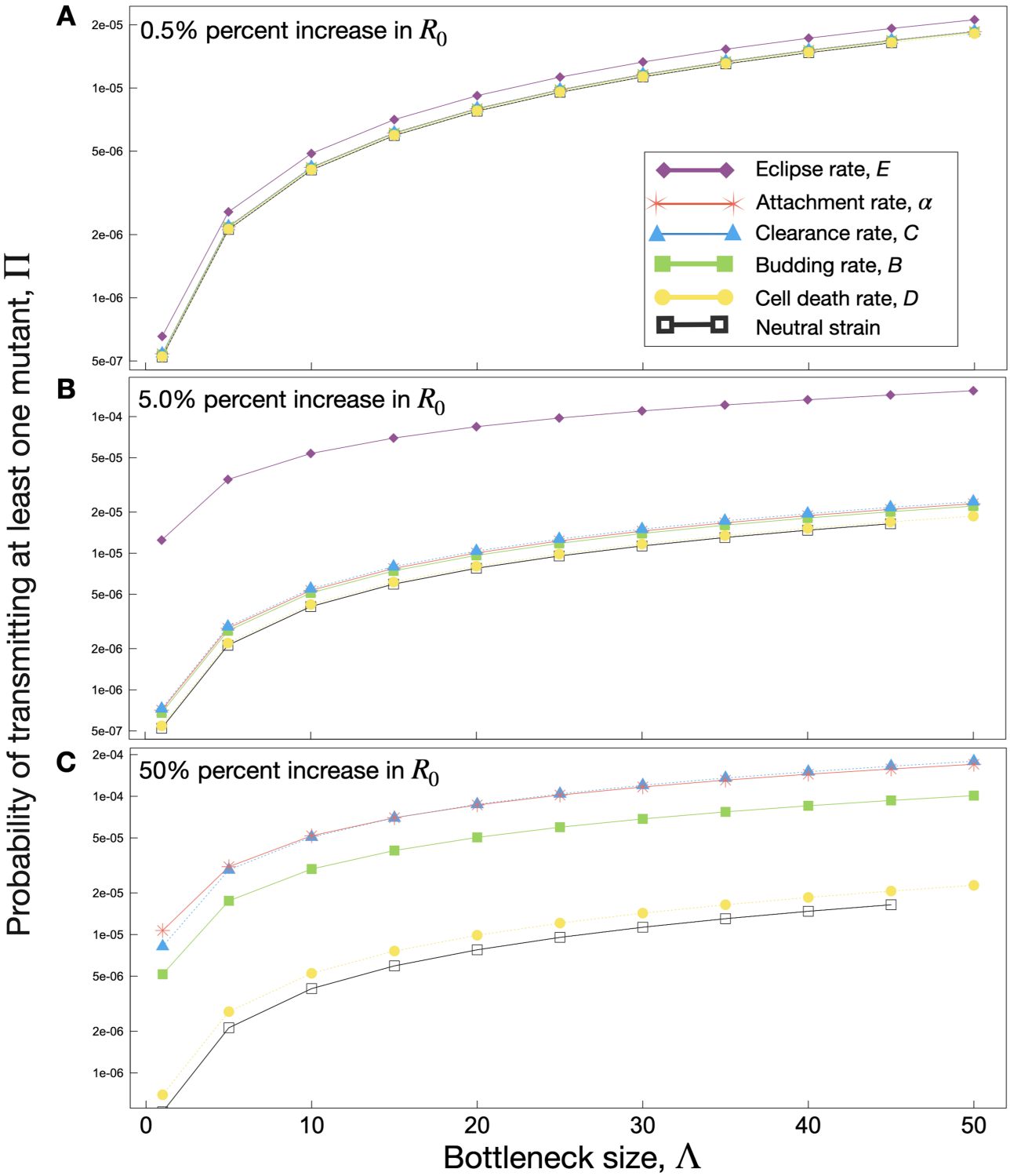

Figure 4. Probability of transmitting at least one copy of a specific mutation, Π (Eq. (S9)), as a function of bottleneck size for selective coefficients 0.5 per cent (A), 5 per cent (B), and 50 per cent (C). E is omitted from (C) as only selective coefficients up to 6.5 per cent were examined for this parameter.

3–4 weeks post–initial infection, the probability of transmitting a single virion carrying a specific mutation is on the order of $10^{-7} - 10^{-6}$ (Fig. 3C from Van Egeren et al. (2021) and illustrated by the boxed region in Fig. 3). While we study transmission at peak viral load, this prediction compares remarkably well to our data-driven analytical estimates at narrow bottlenecks ($\Lambda \leq 5$).

It is important to note that the quantity Π (defined in Eq. (S9)) reflects the probability that a *specific* mutation, with a specific effect, occurs *de novo* during a single infection and is successfully transmitted. As a back-of-the-envelope estimation, we can multiply Π by the length of the SARS-CoV-2 genome and by three possible mutations per site, yielding .045 mutations transmitted

per infection (assuming neutral mutations and a bottleneck of one virion). However, the underlying mutation rate includes all possible non-lethal mutations, a large fraction of which is deleterious and would not, in fact, survive within-host competition and be transmitted. Assuming that 10 per cent of all mutations are non-deleterious (Eyre-Walker and Keightley, 2007), we estimate the probability that at least one beneficial or neutral mutation occurs *de novo* and is passed on as approximately 4×10^{-3} per transmission event. We point out that this estimate is not directly comparable to the substitution rate, a measure of the rate at which mutations accrue globally in SARS-CoV-2 (Markov et al., 2023). To estimate the latter, we would need to further include multiple transmissions per host and the fate of the transmission chain carrying the new mutation, including epidemiological competition among strains, and the (possibly high) chance of epidemiological extinction of the new variant.

If we restrict our results to narrow bottlenecks ($\Lambda = 1$), with transmission probabilities confined to the range of $10^{-7} - 10^{-6}$ (based on (Van Egeren et al., 2021)), the inset of Fig 3 depicts the predicted parameter space for mutants affecting each of the examined parameters and also illustrates the maximum increases in selective coefficients of key viral life history traits. We can see that all mutations reducing infected cell death, D, are within this region. In contrast, mutations affecting the eclipse rate, E, are only included for a maximum increase in R_0 of ~2.5 per cent. Mutations affecting the per target cell attachment rate, α, viral clearance, C, and virion budding rate, B, display a similar response as a function of percent increase in R_0 and are intermediate to D and E. Using 1×10^{-6} as a maximum transmission probability, we can also place limits on the percent change relative to the neutral strain of each of our parameters, leading to a prediction for limitations to likely phenotypic changes caused by a single advantageous mutant. Relative to the neutral strain, we find that parameters α, B, C, D, and E shift R_0 by approximately 10, 11.5, 10, 50.0, and 1 per cent, respectively. These increases in R_0 correspond to percent parameter changes of 18.4, 11.5, 15.5, 32.0, and 19.0 for α, B, C, D, and E, respectively. Thus, by binding the probability of transmission to 1×10^{-6} as suggested by simulation studies (Van Egeren et al., 2021), we can put an upper bound on predicted changes in key phenotypic traits that have arisen from a single mutation.

While the dataset used to inform our within-host model comprises predominantly hospitalized individuals, this dataset was chosen due to the demonstrated identifiability and validity of the within-host parameter estimates (Korosec et al., 2023). In future work, we hope to study the transmission of *de novo* mutations using parameter estimates for mild SARS-CoV-2 infection, once a clear consensus on such parameters has emerged. Given the relatively rapid clearance of viral load during mild SARS-CoV-2, we expect that our current study of more severe infections offers an upper bound on the probability that *de novo* mutations are transmitted. Similarly, our current work ignores any competition between beneficial variants during a single within-host infection. Given the relatively low mutation rate of SARS-CoV-2, the high probability that a new mutation will be deleterious, and the probability that a *de novo* lineage will go extinct while rare, we expect that competition between beneficial lineages will not be a strong factor, but where it occurs it would reduce the chance that any specific mutation is transmitted. Thus, again our approach offers an upper bound and the effect of competition between strains remains to be tested in future work.

Next, we focus on mutations affecting each phenotypic trait individually, examining our predictions in the context of identified SARS-CoV-2 mutations. The predominant structural proteins of SARS-CoV-2 include membrane glycoprotein (M), envelope protein (E), nucleocapsid protein (N), and the spike protein (S) (Thomas, 2020). Mutations in M, E, N, or S can affect various life-history traits captured by our stochastic model describing the fate of mutant lineages (Eq. (2)). We briefly summarize a number of key mutations identified in SARS-CoV-2 VOC in Table 2, with reference to expected changes in our model parameters based on observed phenotypic effects.

The per target cell attachment rate, α, represents a myriad of interactions involved in a virus gaining access to the host-cell intracellular environment (Boulant, Stanifer and Lozach, 2015); from initial binding, diffusion throughout the pericellular domain (Vahey and Fletcher, 2019; Korosec et al., 2021), to fusion, and host-cell entry (Wu et al., 2023). Each of these are complex processes involving a multitude of viral–host interactions. The omicron variant has, for example, been found to have accelerated cilia-dependent cellular entry in nasal epithelia, which contributes to its increased attack rate over previous variants (Wu et al., 2023). Many pre-omicron SARS-CoV-2 mutations are hypothesized to have increased fitness in viral attachment predominantly through enhanced angiotensen-converting enzyme 2 (ACE2) binding affinity achieved through spike and receptor-binding domain (RBD)-specific mutations (Khan et al., 2021; Fratev, 2021; Liu et al., 2022; Ozono et al., 2021) (Table 2). Some mutations, for example, N439K, are found to enhance ACE2 binding and also contribute to humoral immune escape (Thomson et al., 2021). As noted previously, substantial percentage changes in α, relative to changes in the viral clearance or budding rates, are required to achieve the same increase in R_0 (Fig. 2B). If such increases to α are achieved, however, we predict that the transmission probability for mutants with higher attachment rates is very similar to those with higher budding or reduced clearance (Fig. 3), again for the same increase in R_0. Therefore, our work suggests mutations affecting humoral immune evasion (C) and ACE2 binding affinity and fusogenicity (α) to be equally transmittable, assuming that the mutations confer a similar selective advantage. These results also suggest that 'big benefit' changes in binding affinity and fusogenicity are favoured to emerge and be transmitted, as observed in omicron and several pre-omicron variants. Finally, we note that the survival probability (Eq. (S5)) scales with bottleneck size similarly for virion attachment as it does for virion clearance (Fig. S3), demonstrating that these predictions are not sensitive to the size of the transmission bottleneck.

When an infectious virus enters its host cell, it does not instantaneously begin self-replication. Viral production requires a period of time, the eclipse phase, during which the virus manipulates a multitude of cellular processes to facilitate an environment for self-replication and continued transmission (Lozach, 2020). In our model, advantageous mutations affecting the eclipse phase result in a virus more quickly transitioning from host-cell entry through to initial budding, captured through an increased eclipse rate, E. We find advantageous mutations affecting E to confer a high probability of transmission, Π. For example, an increase of 10 per cent in R_0 leads to an order of magnitude increase in Π, where this substantial increase in Π is not seen for any other parameter (Fig. 3). In Fig. 4, showing Π as a function of bottleneck size, we predict that at a 0.5 per cent R_0 increase, favourable eclipse phase mutations have higher chances of transmission than equivalent changes to any other parameter, across any bottleneck size. As R_0 is further increased to 5.0 per cent, advantageous eclipse phase mutations lead to an order of magnitude increase in the probability that the mutation arises during the infection, and at least one

Table 2. Summary of mutations, phenotypic effects, and associated predicted change to within-host model parameter(s).

VOC	Mutation	Phenotypic effect	Model parameter
Alpha	N501Y	Improves spike protein binding to cellular receptors, enhances transmission (Liu et al., 2022) α & percentage; D614G Enhanced viral replication, increased viral fitness (Plante et al., 2021; Ozono et al., 2021)	*B*, *E*
	E484K	Increased evasion of neutralizing antibodies (Jangra et al., 2021; Alenquer et al., 2021)	*C*
	S494P	Increased evasion of neutralizing antibodies (Alenquer et al., 2021)	*C*
	K417N	Increased the RBD-ACE2 free energy of binding, increased infectivity (Fratev, 2021; Khan et al., 2021)	α
Delta	D614G	Enhanced ACE2 binding efficiency (Ozono et al., 2021)	α
	L452R	Evades cellular immunity and increases infectivity (Tchesnokova et al., 2021; Zhang et al., 2022; Motozono et al., 2021)	*D*
	T478K	Potentially hinders receptor binding, contributes to immune escape (Di Giacomo et al., 2021; Wilhelm et al., 2021)	*D*, *C*
	I82T	Affects viral assembly and inhibits interferon-gamma (IFN_γ) (Shen et al., 2021)	*E*, *B*, *D*
	P681H	Confers type I interferon resistance (Lista et al., 2022)	*D*, α
Omicron	Q493R, Q498R, and Y501H	Hypothesized to increase binding affinity to negatively charged HSPGs present on the cell surface (Nie et al., 2022)	α
	I189V	Inhibits IFN_γ signalling (Bills et al., 2023)	*D*
	T19I, L24S, del25–27, G142D, and del143-145	N-terminal domain mutations causing significant evasion from nABs (Xia et al., 2022; Fan et al., 2022)	*C*
	H655Y	Enhances viral fusogenicity (Escalera et al., 2022)	α
	P681R	Enhances viral fusogenicity (Saito et al., 2022)	α
BA.4 specific	L452R, F486V	Increased immune evasion, linked to breakthrough infections (Xia et al., 2022; Zhang et al., 2022)	*C*, *D*
BA.4-BA.5 specific	L452Q/R	Linked to significant humoral immunity escape (Cao et al., 2022)	*C*
BA.2.12.1-specific	L452Q	Increased immune evasion, linked to breakthrough infections (Xia et al., 2022; Zhang et al., 2021)	*C*, *D*

copy survives to be transmitted, Π, for all bottleneck sizes, Λ, as compared to all other parameters.

Putting this prediction in context, we note that one of the major components of the host-cell infection process is to reprogram cell metabolic processes, typically in the form of increased glycolysis (Vigerust and Shepherd, 2007) and hijacking of glucose transport pathways (Thaker et al., 2019). The SARS-CoV-2 M protein, the most abundant of the structural proteins (Marques-Pereira et al., 2022), has been found to be homologous to the prokaryotic sugar transport protein SemiSWEET and is further hypothesized to be implicated in proliferation, replication, and immune evasion (Thomas, 2020). Utilizing SARS-CoV-2 genomic surveillance data from 2020, with phylogenetic analyses carried out via Nextstrain (Hadfield et al., 2018), (Shen et al., 2021) associate the rapid emergence of the B.1.575 lineage with mutations in the M protein. They relate the mutations in the M protein to more advantageous glucose uptake during viral assembly (Shen et al., 2021). In our model, this M mutation can be captured by advantageous mutations in the eclipse parameter, *E*, and/or the budding rate, *B*, as the mutation is hypothesized to lead to a more optimal within-cell replication and viral proliferation. In other modelling work, SARS-CoV-2 viral load has been shown to be highly sensitive to the eclipse duration; thus, mutations affecting the ability to more quickly reprogram intracellular machinery would be highly favourable (Pearson et al., 2023). It is therefore possible that our eclipse mutation results (Fig. 3), with neutral strain properties (Korosec et al., 2023) determined from SARS-CoV-2 data gathered at a similar time as the study by Shen et al. (2021), are revealing the high probability of such a mutation to emerge at this time of the pandemic, and this result further supports the importance of therapeutics that target the M protein (Marques-Pereira et al., 2022).

Qualitatively, why are mutations that reduce the eclipse phase so different from the mutations affecting other traits in this model? As mentioned previously, at the parameter values, we study (for severe SARS-CoV-2 infections) the eclipse phase that lasts for less than 5 h, whereas an infected cell lives, on average, for about 3 days. Thus, reductions to the eclipse phase have a limited overall effect on the within-host R_0. Recall, however, that R_0 measures the overall number of copies produced by a single viral particle, but captures no information about the timing of this reproduction (Heffernan, Smith and Wahl, 2005). A viral strain that produces twenty infectious copies has the same R_0 value, whether those copies are produced in 3 days or in 3 h. In contrast, the successful transmission of a new variant depends critically on timing. The rapid exponential growth of viral load within a single individual constitutes an environment of extreme competitive selection. Thus, any mutation that colonizes the available target cells more quickly has a tremendous advantage in the time-limited within-host competition and therefore a tremendous transmission advantage.

The result that beneficial mutations in *E* have an increased probability of transmission, as compared to mutations in other parameters resulting in a similar selective coefficient, is therefore not surprising. It is known that a shorter eclipse phase has a higher intrinsic growth rate during the expansion phase because of its shorter generation interval (Wallinga and Lipsitch, 2007). The result we reveal in this work for SARS-CoV-2, based on data collected from February 2020 through to February 2021 (and thus mostly composed of wild-type and B117 variants), is

that mutations that reduce the eclipse phase mean duration have nearly an order of magnitude higher transmission probability as compared to mutations in all other examined traits with equivalent selective coefficients. We would thus predict that mutations leading to shorter generation intervals should have had significantly higher selective pressure as compared to other phenotypic changes. This result appears to be well supported by analysis of generation intervals between the Delta and Omicron variants. It was initially reported that the Omicron variant had a shorter incubation period and shorter generation interval than compared to the Delta variant (Backer et al., 2022). Upon careful reanalysis of the data accounting for a dynamical bias of observing faster transmission in an early epidemic scenario, it was determined that the incubation period of Omicron is similar to Delta; however, Omicron exhibits a significantly shorter generation interval (Park et al., 2023). This is entirely consistent with our model prediction that mutations increasing E are strongly favoured to emerge.

SARS-CoV-2 mutations affecting immune escape have been of paramount interest throughout the pandemic (Callaway, 2021; Harari et al., 2022; Starr et al., 2021) and are of key importance towards understanding and predicting vaccine efficacy against emerging variants (Chakraborty et al., 2022; Ao et al., 2022). Single mutations in M, E, N, or S can have complex outcomes with multiple phenotypic changes (Thomson et al., 2021). S mutations, for example, have been linked not only to enhanced viral entry (L5F) but also to increased resistance to antibodies (G446V and A879V) (Lythgoe et al., 2021). In our model, mutations enhancing immune escape could be captured by cell death, D, or viral load clearance, C. Mutations affecting D will include phenotypic outcomes associated with recognition or killing of infected cells, avoiding recognition by the immune system, or, if we extended the model to include a time-varying death rate, reducing the innate immune response. For example, the Alpha-variant mutations to Orf9b are associated with suppression of the innate immune response through reduced interferon induction (Thorne et al., 2022); such a change in viral dynamics could be captured by parameter D in our model. Advantageous mutations leading to humoral evasion are captured by decreases in the viral load clearance rate. For example, the BA.4 and BA.5 subvariants have been found to exhibit humoral evasion (Jian et al., 2022) and thus would exhibit a lower rate of virion clearance as compared to previous mutants.

We find mutants affecting D to have little impact on predicted survival probabilities (P_s, Eq. (S5)) for all bottleneck sizes (Fig. S3D) and lead to transmission probabilities nearly equivalent to the neutral strain for all selective coefficients and bottleneck sizes we examined (Figs. S5 and 4). In contrast, mutations in virion clearance scale similar to target cell attachment (Figs. S5, 4, and S6C) exhibit large increases in P_s as a function of increased bottleneck size for any particular t_m (Fig. S3C). This point is also made clear through a simple calculation of maximum predicted Π achieved for each parameter at narrow bottlenecks ($\Lambda = 1$). The percent difference in D required to achieve a 50 per cent increase in R_0 is 32 per cent and results in an increase in Π of a factor of 1.3 relative to the neutral strain. In contrast, the percent difference in C required to achieve a 50 per cent percent increase in R_0 is 57 per cent and results in an increase in Π of a factor of 15.1 relative to the neutral strain. Our results predict that advantageous mutations leading to humoral escape have a significantly higher probability to be transmitted to the next host, as compared to mutations associated with recognition or killing of infected cells. Once again, we argue that this prediction emerges due to timing considerations during the intense competition within the host. Evading humoral escape, such that a greater fraction of infectious virions successfully attach to new target cells, allows for a more rapid colonization of the respiratory tract and thus improves the chance that a variant is transmitted. In contrast, when an infected cell lives longer, the total output of infectious virions is increased by extending the time at which these virions emerge. Thus, in the first case, the infection proceeds more rapidly while in the second, R_0 is increased without a concomitant change in timing. This could explain our prediction that mutations leading to humoral escape are more likely to emerge than mutations that escape the recognition and death of infected cells.

We also note, however, that if we restrict our results to an experimentally estimated Π range of $10^{-7} - 10^{-6}$ (boxed region, Fig .3), then the entire explored parameter space for D falls within the region, while only a limited region of parameter space for C does. Thus, although mutations in C confer a significantly higher transmission advantage, there appears to be significantly more explorable parameter space for mutations affecting D.

Finally, shown in Fig. S5 is an alternative visualization of these results, in which all the curves in Fig .4 are normalized by the neutral strain probability. Here, we see that at a 5.0 per cent R_0 increase (Figure S5B), for narrow bottlenecks, Π exceeds 20 times the neutral strain value. As bottleneck size is increased, the neutral-normalized Π decreases monotonically such that at $\Lambda = 50$, Π has decreased to ~10 times the neutral strain value. Thus, we uncover that one outcome of increasing bottleneck size is to monotonically reduce the probability of transmission relative to the neutral strain. This effect is particularly apparent for mutations affecting the eclipse period; however, this trend can be observed with all other parameters as well. This result, which emerges from our analytical approach (Eq. (2)), suggests that small bottleneck sizes (Martin and Koelle, 2023; Bendall et al., 2023) favour the adaptive evolution of SARS-CoV-2, as we find that narrow bottleneck sizes ($\Lambda < 5$) increase the transmission probability for adaptive, as compared to neutral, phenotypic changes.

In this work, our within-host modelling approach is based on severe infection of the upper respiratory tract (URT), without including potential implications of spatial inhomogeneities or spatially dependent bottleneck dynamics. *In vivo* modelling studies that consider the entire human respiratory tract have been developed for influenza (Quirouette et al., 2020) and would be of interest for application to SARS-CoV-2 infection. For other diseases, such as human rhinovirus, it has recently been found that infections that progress from the URT to the lower respiratory tract (LRT) contain no specific evolutionary requirement (Makhsous et al., 2023); however, an equivalent study on SARS-CoV-2 does not exist to our knowledge. Within-host modelling studies on URT and LRT of SARS-CoV-2 infection have found dramatic differences in reproduction number and intrahost dynamics and further suggest that long-term COVID infections are sustained by continuous infection of new target cells within the LRT (Ke et al., 2020). Indeed, intrahost genetic diversity in chronic infections lasting over a year reveals accelerated virus evolutionary rates (Chaguza et al., 2023) and emergence of strains resistant to monoclonal antibodies (mABs) (Halfmann et al., 2023). Prolonged viral shedding in immunocompromised individuals has also been correlated with the emergence of immune escape mutations (Sonnleitner et al., 2022; Quaranta et al., 2022). Future considerations of transmission bottleneck dynamic timescales beyond peak viral load for long-term infections, with within-host

infection dynamics corresponding to sustained infection, would therefore be of interest.

In summary, our work examines the probability that a novel mutation emerges during a single SARS-CoV-2 infection and is transmitted to a subsequent host. Comparing mutations that have the same overall effect on R_0, we predict that phenotypic changes allowing for more rapid within-host colonization are strongly favoured for transmission. Our focus on neutral and beneficial mutations is consistent with recent longitudinal analyses of intrahost single-nucleotide variants of SARS-CoV-2, which demonstrate a strong signal of positive selection acting on these variants (Li et al., 2022). Once a new variant is transmitted, however, other traits may be critical for establishment in the new host; our approach does not address this establishment probability. Given recent evidence of negative selection (a reduced fraction of non-synonymous mutations) at this transmission stage (Li et al., 2022), pleiotropic trade-offs between within-host replication rate and between-host establishment may be relevant for SARS-CoV-2 and will be an important direction for future modelling.

Data availability

The datasets generated during and/or analysed during the current study are available from the corresponding author on reasonable request. The code required to reproduce the main body of results can be found in a publicly available GitHub page sourced at https://github.com/chapSKor/Bottleneck_VirusEvolution.

Supplementary data

Supplementary data are available at *Virus Evolution* online.

Acknowledgements

C.S.K. acknowledges Natural Sciences and Engineering Research Council of Canada (NSERC) Postdoctoral funding. L.M.W. and J.M.H. are funded by NSERC. J.M.H. acknowledges support from the York University Research Chair Program, the Canadian Insitutes for Health Research (CIHR) and the NSERC-Public Health Agency of Canada Emerging Infectious Disease Modelling initiative.

References

Agostini, M. L. et al. (2018) 'Coronavirus susceptibility to the antiviral remdesivir (GS-5734) is mediated by the viral polymerase and the proofreading exoribonuclease', *MBio*, 9: 10–1128.

Alenquer, M. et al. (2021) 'Signatures in SARS-CoV-2 spike protein conferring escape to neutralizing antibodies', *PLOS Pathogens*, 17: e1009772.

Amicone, M. et al. (2022) 'Mutation rate of SARS-CoV-2 and emergence of mutators during experimental evolution', *Evolution, Medicine and Public Health*, 10: 142–155.

Ao, D. et al. (2022) 'SARS-CoV-2 Omicron variant: Immune escape and vaccine development', *MedComm*, 3: e126.

Baccam, P. et al. (2006) 'Kinetics of Influenza A Virus Infection in Humans', *Journal of Virology*, 80: 7590–7599.

Backer, J. A. et al. (2022) 'Shorter serial intervals in SARS-CoV-2 cases with Omicron BA. 1 variant compared with Delta variant, the Netherlands, 13 to 26 December 2021', *Eurosurveillance*, 27: 2200042.

Bendall, E. E. et al. (2023) 'Rapid transmission and tight bottlenecks constrain the evolution of highly transmissible SARS-CoV-2 variants', *Nature Communications*, 14: 1–7.

Betti, M. et al. (2021) 'Integrated vaccination and non-pharmaceutical interventions based strategies in Ontario, Canada, as a case study: a mathematical modelling study', *Journal of The Royal Society Interface*, 18: 20210009.

Bills, C. J. et al. (2023) 'Mutations in SARS-CoV-2 variant nsp6 enhance type-I interferon antagonism', *Emerging Microbes and Infections (just-accepted).*, 12: 2209208.

Boulant, S., M., Stanifer and P. Y., Lozach (2015) 'Dynamics of virus-receptor interactions in virus binding, signalin. and endocytosis', *Viruses*, 7: 2794–815.

Braun, K. M. et al. (2021) 'Acute SARS-CoV-2 infections harbor limited within-host diversity and transmit via tight transmission bottlenecks', *PLoS Pathogens*, 17: 1–26.

Callaway, E. (2021) 'Beyond Omicron: What's next for SARS-CoV-2 Evolution', *Nature*, 600: 204–7.

Cao, Y. et al. (2021) 'Immune-viral dynamics modeling for SARS-CoV-2 drug development', *Clinical and Translational Science*, 14: 2348–59.

Cao, Y. et al. (2022) 'BA.2.12.1, BA.4 and BA.5 escape antibodies elicited by Omicron infection', *Nature*, 608: 593–602.

Chaguza, C. et al. (2023) 'Accelerated SARS-CoV-2 intrahost evolution leading to distinct genotypes during chronic infection', *Cell Reports Medicine*, 4.

Chakraborty, C. et al. (2022) 'A detailed overview of immune escape, antibody escape, partial vaccine escape of SARS-CoV-2 and their emerging variants with escape mutations', *Frontiers in Immunology*, 13: 801522.

Ciupe, S. M. and N., Tuncer (2022) 'Identifiability of parameters in mathematical models of SARS-CoV-2 infections in humans', *Scientific Reports*, 12: 14637.

Di Giacomo, S. et al. (2021) 'Preliminary report on severe acute respiratory syndrome coronavirus 2 (SARS-CoV-2) Spike mutation T478K', *Journal of Medical Virology*, 93: 5638–43.

Escalera, A. et al. (2022) 'Mutations in SARS-CoV-2 variants of concern link to increased spike cleavage and virus transmission', *Cell Host and microbe*, 30: 373–87.

Eyre-Walker, A. and P. D., Keightley (2007) 'The distribution of fitness effects of new mutations', *Nature Reviews Genetics*, 8: 610–8.

Fan, Y. et al. (2022) 'SARS-CoV-2 Omicron variant: recent progress and future perspectives', *Signal Transduction and Targeted therapy*, 7: 141.

Farhang-sardroodi, S. et al. (2021) 'Analysis of Host Immunological Response of Adenovirus-Based COVID-19 Vaccines', *Vaccines*, 9: 861.

Fratev, F. (2021) 'N501Y and K417N mutations in the spike protein of SARS-CoV-2 alter the interactions with both hACE2 and human-derived antibody: a free energy of perturbation retrospective study', *Journal of Chemical Information and Modeling*, 61: 6079–84.

Gholami, S. et al. (2023) 'A mathematical model of protein subunits COVID-19 vaccines', *Mathematical Biosciences*, 358: 108970.

Ghosh, S. et al. (2020) 'β-Coronaviruses Use Lysosomes for Egress Instead of the Biosynthetic Secretory Pathway', *Cell*, 183: 1520–35.

Gonçalves, A. et al. (2020) 'Timing of Antiviral Treatment Initiation is Critical to Reduce SARS-CoV-2 Viral Load', *CPT: Pharmacometrics and Systems Pharmacology*, 9: 509–14.

Gonçalves, A. et al. (2021) 'SARS-CoV-2 viral dynamics in non-human primates', *PLoS Computational Biology*, 17: e1008785.

Goyal, A., E. F., Cardozo-Ojeda and J. T., Schiffer (2020) 'Potency and timing of antiviral therapy as determinants of duration of SARS-CoV-2 shedding and intensity of inflammatory response', *Science Advances*, 6: eabc7112.

Hadfield, J. et al. (2018) 'Nextstrain: real-time tracking of pathogen evolution', *Bioinformatics*, 34: 4121–23.

Halfmann, P. J. et al. (2023) 'Evolution of a globally unique SARS-CoV-2 Spike E484T monoclonal antibody escape mutation in a persistently infected, immunocompromised individual', *Virus Evolution*, 9: veac104.

Harari, S. et al. (2022) 'Drivers of adaptive evolution during chronic SARS-CoV-2 infections', *Nature Medicine*, 28: 1501–8.

Heffernan, J. M., R. J., Smith and L. M., Wahl (2005) 'Perspectives on the basic reproductive ratio', *Journal of the Royal Society Interface*, 2: 281–93.

Jangra, S. et al. (2021) 'SARS-CoV-2 spike E484K mutation reduces antibody neutralisation', *The Lancet Microbe*, 2: 283–4.

Jian, F. et al. (2022) *Further humoral immunity evasion of emerging SARS-CoV-2 BA.4 and BA.5 subvariants*.

Johansson, M. A. et al. (2021) 'SARS-CoV-2 transmission from people without COVID-19 symptoms', *JAMA Network open*, 4: 2035057.

Jones, T. C. et al. (2021) 'Estimating infectiousness throughout SARS-CoV-2 infection course', *Science*, 373: eabi5273.

Ke, R. et al. (2020) 'Kinetics of SARS-CoV-2 infection in the human upper and lower respiratory tracts and their relationship with infectiousness', *MedRxi*, 2020–09.

Khan, A. et al. (2021) 'Higher infectivity of the SARS-CoV-2 new variants is associated with K417N/T, E484K, and N501Y mutants: an insight from structural data', *Journal of Cellular physiology*, 236: 7045–57.

Korosec, C. S. et al. (2021) 'Substrate stiffness tunes the dynamics of polyvalent rolling motors', *Soft Matter*, 17: 1468–79.

Korosec, C. S. et al. (2022) 'Long-term durability of immune responses to the BNT162b2 and mRNA-1273 vaccines based on dosage, age and sex', *Scientific Reports*, 12: 21232.

Korosec, C. S. et al. (2023) 'Multiple cohort study of hospitalized SARS-CoV-2 in-host infection dynamics: Parameter estimates, identifiability, sensitivity and the eclipse phase profile', *Journal of Theoretical biology*, 564: 111449.

Le Rutte, E. A. et al. (2022) 'Modelling the impact of Omicron and emerging variants on SARS-CoV-2 transmission and public health burden', *Communications Medicine*, 2: 93.

Li, J. et al. (2022) 'Two-step fitness selection for intra-host variations in SARS-CoV-2', *Cell Reports*, 38.

Lin, J. et al. (2022) 'Longitudinal Assessment of SARS-CoV-2-Specific T Cell Cytokine-Producing Responses for 1 Year Reveals Persistence of Multicytokine Proliferative Responses, with Greater Immunity Associated with Disease Severity', *Journal of Virology*, 96: 00509–22.

Lista, M. J. et al. (2022) 'The P681H mutation in the spike glycoprotein of the alpha variant of SARS-CoV-2 escapes IFITM restriction and is necessary for type I interferon resistance', *Journal of virology*, 96: 01250–22.

Liu, X. et al. (2021) 'Disruption of respiratory epithelial basement membrane in COVID-19 patients', *Molecular biomedicine*, 2: 1–4.

Liu, Y. et al. (2022) 'The N501Y spike substitution enhances SARS-CoV-2 infection and transmission', *Nature*, 602: 294–9.

Longdon, B. et al. (2015) 'The Causes and Consequences of Changes in Virulence following Pathogen Host Shifts', *PLoS Pathogens*, 11: 1–18.

Lozach, P. -Y. (2020) 'Cell Biology of Viral Infections', *Cells*, 9: 2431.

Lythgoe, K. A. et al. (2021) 'SARS-CoV-2 within-host diversity and transmission', *Science*, 372: eabg0821.

Makhsous, N. et al. (2023) 'Within-Host Rhinovirus Evolution in Upper and Lower Respiratory Tract Highlights Capsid Variability and Mutation-Independent Compartmentalization', *bioRxiv*.

Markov, P. V. et al. (2023) 'The evolution of SARS-CoV-2', *Nature Reviews Microbiology*, 21: 361–78.

Marques-Pereira, C. et al. (2022) 'SARS-CoV-2 Membrane Protein: From Genomic Data to Structural New Insights', *International Journal of Molecular Sciences*, 23: 2986.

Martin, M. A. and K., Koelle (2023) 'Comment on "Genomic epidemiology of superspreading events in Austria reveals mutational dynamics and transmission properties of SARS-CoV-2"', *Science Translational Medicine*, 13: eabh1803.

Matveev, V. A. et al. (2023) 'Immunogenicity of COVID-19 vaccines and their effect on HIV reservoir in older people with HIV', *iScience*, 26: 107915.

Motozono, C. et al. (2021) 'SARS-CoV-2 spike L452R variant evades cellular immunity and increases infectivity', *Cell Host and microbe*, 29: 1124–36.

Moyles, I. R., C. S., Korosec and J. M., Heffernan (2023) 'Determination of significant immunological timescales from mRNA-LNP-based vaccines in humans', *Journal of Mathematical Biology*, 86: 1–41.

Néant, N. et al. (2021) 'Modeling SARS-CoV-2 viral kinetics and association with mortality in hospitalized patients from the French COVID cohort', *PNAS*, 118: e2017962118.

Nie, C. et al. (2022) 'Charge matters: Mutations in omicron variant favor binding to cells', *ChemBioChem*, 23: e202100681.

Ozono, S. et al. (2021) 'SARS-CoV-2 D614G spike mutation increases entry efficiency with enhanced ACE2-binding affinity', *Nature communications*, 12: 848.

Padmanabhan, P., R., Desikan and N. M., Dixit (2022) 'Modeling how antibody responses may determine the efficacy of COVID-19 vaccines', *Nature Computational Science*, 2: 123–31.

Park, S. W. et al. (2023) 'Inferring the differences in incubation-period and generation-interval distributions of the Delta and Omicron variants of SARS-CoV-2', *Proceedings of the National Academy of Sciences of the United States of America*, 120: 1–12.

Pearson, J. et al. (2023) 'Modeling identifies variability in SARS-CoV-2 uptake and eclipse phase by infected cells as principal drivers of extreme variability in nasal viral load in the 48 h post infection', *Journal of Theoretical biology*, 565: 111470.

Perelson, A. S. and R., Ke (2021) 'Mechanistic Modeling of SARS-CoV-2 and Other Infectious Diseases and the Effects of Therapeutics', *Clinical Pharmacology and Therapeutics*, 109: 829–40.

Plante, J. A. et al. (2021) 'Spike mutation D614G alters SARS-CoV-2 fitness', *Nature*, 592: 116–21.

Quaranta, E. G. et al. (2022) 'SARS-CoV-2 intra-host evolution during prolonged infection in an immunocompromised patient', *International Journal of Infectious Diseases*, 122: 444–8.

Quirouette, C. et al. (2020) 'A mathematical model describing the localization and spread of influenza A virus infection within the human respiratory tract', *PLOS Computational Biology*, 16: e1007705.

Rambaut, A. et al. (2020) 'A dynamic nomenclature proposal for SARS-CoV-2 lineages to assist genomic epidemiology', *Nature Microbiology*, 5: 1403–7.

Ramphal, R. et al. (1979) 'Murine influenzal tracheitis: a model for the study of influenza and tracheal epithelial repair', *American Review of Respiratory Disease*, 120: 1313–24.

Saito, A. et al. (2022) 'Enhanced fusogenicity and pathogenicity of SARS-CoV-2 Delta P681R mutation', *Nature*, 602: 300–6.

Salzberger, B. et al. (2021) 'Epidemiology of SARS-CoV-2', *Infection*, 49: 233–9.

Schaefer, I. M. et al. (2020) 'In situ detection of SARS-CoV-2 in lungs and airways of patients with COVID-19', *Modern Pathology*, 33: 2104–14.

Sette, A. and S., Crotty (2021) 'Adaptive immunity to SARS-CoV-2 and COVID-19', *Cell*, 184: 861–80.

Shen, L. et al. (2021) 'Emerging variants of concern in SARS-CoV-2 membrane protein: a highly conserved target with potential pathological and therapeutic implications', *Emerging Microbes and Infections*, 1010: 885–93.

Shen, L. et al. (2021) 'Emerging variants of concern in SARS-CoV-2 membrane protein: a highly conserved target with potential pathological and therapeutic implications', *Emerging Microbes and Infections*, 11: 885–93.

Sigal, D., J. N. S., Reid and L. M., Wahl (2018) 'Effects of transmission bottlenecks on the diversity of influenza a virus', *Genetics*, 210: 1075–88.

Sonnleitner, S. T. et al. (2022) 'Cumulative SARS-CoV-2 mutations and corresponding changes in immunity in an immunocompromised patient indicate viral evolution within the host', *Nature Communications*, 13: 2560.

Starr, T. N. et al. (2021) 'Prospective mapping of viral mutations that escape antibodies used to treat COVID-19', *Science*, 371: 850–4.

Tchesnokova, V. et al. (2021) 'Acquisition of the L452R mutation in the ACE2-binding interface of Spike protein triggers recent massive expansion of SARS-Cov-2 variants', *Journal of Clinical microbiology*, 59: 00921–21.

Thaker, S. K., J., Ch'ng and H. R., Christofk (2019) 'Viral hijacking of cellular metabolism', *BMC biology*, 17: 1–15.

Thomas, S. (2020) 'The Structure of the Membrane Protein of SARS-CoV-2 Resembles the Sugar Transporter SemiSWEET', *Pathogens and Immunity*, 5: 342–63.

Thomson, E. C. et al. (2021) 'Circulating SARS-CoV-2 spike N439K variants maintain fitness while evading antibody-mediated immunity', *Cell*, 184: 1171–87.

Thorne, L. G. et al. (2022) 'Evolution of enhanced innate immune evasion by SARS-CoV-2', *Nature*, 602: 487–95.

Tian, D. et al. (2022) 'The emergence and epidemic characteristics of the highly mutated SARS-CoV-2 Omicron variant', *Journal of Medical virology*, 94: 2376–83.

Vahey, M. D. and D. A., Fletcher (2019) 'Influenza a virus surface proteins are organized to help penetrate host mucus', *Elife*, 8: e43764.

Vaira, L. A. et al. (2020) 'Olfactory epithelium histopathological findings in long-term coronavirus disease 2019 related anosmia', *The Journal of Laryngology and otology*, 134: 1123–7.

Van Egeren, D. et al. (2021) 'Controlling long-term SARS-CoV-2 infections can slow viral evolution and reduce the risk of treatment failure', *Scientific Reports*, 11: 1–9.

Vigerust, D. J. and V. L., Shepherd (2007) 'Virus glycosylation: role in virulence and immune interactions', *Trends in microbiology*, 15: 211–18.

Wallinga, J. and M., Lipsitch (2007) 'How generation intervals shape the relationship between growth rates and reproductive numbers', *Proceedings of the Royal Society B: Biological Sciences*, 274: 599–604.

Wang, D. et al. (2021) 'Population Bottlenecks and Intra-host Evolution During Human-to-Human Transmission of SARS-CoV-2', *Frontiers in Medicine*, 8: 1–7.

WHO Coronavirus (COVID-19) Dashboard (2023). World Health Organization.

Wilhelm, A. et al. (2021) 'Antibody-mediated neutralization of authentic SARS-CoV-2 B. 1.617 variants harboring L452R and T478K/E484Q', *Viruses*, 13: 1693.

Wu, C. T. et al. (2023) 'SARS-CoV-2 replication in airway epithelia requires motile cilia and microvillar reprogramming', *Cell*, 186: 112–30.

XBB.1.5 Updated Risk Assessment (2023) *World Health Organization*. 24 February 2023.

Xia, S. et al. (2022) 'Origin, virological features, immune evasion and intervention of SARS-CoV-2 Omicron sublineages', *Signal Transduction and Targeted Therapy*, 7: 241.

Zhang, C. et al. (2020) 'Clinical and epidemiological characteristics of pediatric SARS-CoV-2 infections in China: A multicenter case series', *PLoS medicine*, 17: e1003130.

Zhang, X. et al. (2021) 'SARS-CoV-2 Omicron strain exhibits potent capabilities for immune evasion and viral entrance', *Signal Transduction and Targeted therapy*, 6: 430.

Zhang, Y. et al. (2022) 'SARS-CoV-2 spike L452R mutation increases Omicron variant fusogenicity and infectivity as well as host glycolysis', *Signal Transduction and Targeted Therapy*, 7: 76.

Virus Evolution, 2024, **10(1)**, 1–12
DOI: https://doi.org/10.1093/ve/veae006
Advance Access Publication 21 February 2024
Research article